Journal of Controlled Release 328 (2020) 942–951

Contents lists available at ScienceDirect

Journal of Controlled Release

journal homepage: www.elsevier.com/locate/jconrel

Correlation between *in vitro* stability and pharmacokinetics of poly (ε-caprolactone)-based micelles loaded with a photosensitizer

Yanna Liu [a], Marcel H.A.M. Fens [a], Robin Bruno Capomaccio [b], Dora Mehn [b], Luca Scrivano [a], Robbert J. Kok [a], Sabrina Oliveira [a,c], Wim E. Hennink [a], Cornelus F. van Nostrum [a,*]

[a] Department of Pharmaceutics, Utrecht Institute for Pharmaceutical Sciences, Utrecht University, Utrecht, the Netherlands
[b] European Commission, Joint Research Centre, Ispra, Italy
[c] Division of Cell Biology, Neurobiology and Biophysics, Department of Biology, Utrecht University, Utrecht, the Netherlands

ARTICLE INFO

Keywords:
Polymer micelles
Drug delivery
in vitro stability
Circulation kinetics
Tumor accumulation

ABSTRACT

Polymeric micelles are extensively investigated as drug delivery systems for hydrophobic drugs including photosensitizers (PSs). In order to benefit from micelles as targeted delivery systems for PS, rather than only solubilizers, the stability and cargo retention of the (PS-loaded) micelles should be properly assessed in biologically relevant media to get insight into the essential parameters predicting their *in vivo* performance (*i.e.,* pharmacokinetics). In the present study, asymmetric flow field-flow fractionation (AF4) was used to investigate the *in vitro* stability in human plasma of empty and meta-tetra(hydroxyphenyl)chlorin (mTHPC)-loaded dithiolane-crosslinked micelles based on poly(ε-caprolactone)-*co*-poly(1,2-dithiolane-carbonate)-*b*-poly(ethylene glycol) (p(CL-*co*-DTC)-PEG) and non (covalently)-crosslinked micelles composed of poly(ε-caprolactone)-*b*-poly (ethylene glycol) (pCL-PEG). AF4 allows separation of the micelles from plasma proteins, which showed that small non (covalently)-crosslinked pCL_9-PEG (17 nm) and pCL_{15}-PEG (22 nm) micelles had lower stability in plasma than pCL_{23}-PEG micelles with larger size (43 nm) and higher degree of crystallinity of pCL, and had also lower stability than covalently crosslinked p(CL_9-$DTC_{3.9}$)-PEG and p(CL_{18}-$DTC_{7.5}$)-PEG micelles with similar small sizes (~20 nm). In addition, PS (re)distribution to specific plasma proteins was observed by AF4, giving strong indications for the (in)stability of PS-loaded micelles in plasma. Nevertheless, fluorescence spectroscopy in human plasma showed that the retention of mTHPC in non (covalently)-crosslinked but semi-crystalline pCL_{23}-PEG micelles (>8 h) was much longer than that in covalently crosslinked p(CL_{18}-$DTC_{7.5}$)-PEG micelles (~4 h). In line with this, *in vivo* circulation kinetics showed that pCL_{23}-PEG micelles loaded with mTHPC had significantly longer half-life values (t½-β of micelles and mTHPC was 14 and 18 h, respectively) than covalently crosslinked p(CL_{18}-$DTC_{7.5}$)-PEG micelles (t½-β of both micelles and mTHPC was ~2 h). As a consequence, long circulating pCL_{23}-PEG micelles resulted in significantly higher tumor accumulation of both the micelles and loaded mTHPC as compared to short circulating p(CL_{18}-$DTC_{7.5}$)-PEG micelles. These *in vivo* data were in good agreement with the *in vitro* stability studies.

In conclusion, the present study points out that AF4 and fluorescence spectroscopy are excellent tools to evaluate the (in)stability of nanoparticles in biological media and thus predict the (in)stability of drug loaded nanoparticles after *i.v.* administration, which is favorable to screen promising delivery systems with reduced experimental time and costs and without excessive use of animals.

1. Introduction

Photosensitizers (PSs) are compounds that are activated by absorbed light to the excited state, following by release of its energy to dissolved oxygen to yield singlet oxygen species, which in turn cause cell death [1,2]. This process is exploited in so-called photodynamic therapy (PDT), a modality that has been clinically approved for treatment of different types of cancer [3,4]. However, some pharmaceutical properties of PSs need optimization to fully exploit their anti-cancer efficacy by PDT. For instance, m-tetra(hydroxyphenyl)chlorin (mTHPC) is a clinically approved second generation PS [5–7]. However, its very hydrophobic character (log P of ~9 [8]) encounters obstacles similar to that of

* Corresponding author.
E-mail address: C.F.vannostrum@uu.nl (C.F. van Nostrum).

https://doi.org/10.1016/j.jconrel.2020.10.040
Received 23 July 2020; Received in revised form 9 October 2020; Accepted 17 October 2020
Available online 22 October 2020

many other PSs and (extremely) hydrophobic chemotherapeutic drugs, such as extremely low-aqueous solubility, aggregation in aqueous media and limited tumor specificity [4,9,10].

Polymeric micelles have the capacity to accommodate hydrophobic PS to yield nanomedicines facilitating its administration and increase accumulation at target tissues *via* passive targeting *(i.e.* enhanced permeability and retention (EPR) effect) and/or direct targeting towards *e.g.* specific receptors or epitopes preferentially (over)-expressed on target cells [4,11–15]. Indeed, as demonstrated in our previous publications [16,17], mTHPC can be solubilized in poly(ε-caprolactone)-*b*-poly(ethylene glycol) (pCL-PEG) based polymeric micelles. In order to exploit the potential of polymeric micelles as targeted delivery systems for PS, these drug carrier systems must have sufficient stability and simultaneously good cargo retention in the circulation [18–21]. However, rapid release of their cargo in the circulation after intravenous (*i.v.*) administration of polymeric micelles loaded with mTHPC or other drugs was observed in previous studies [16,22,23]. This can be likely ascribed to interactions of the micelle-forming block copolymer unimers and/or loaded PS with blood constituents among which plasma proteins [24–29]. Therefore, advanced *in vitro* methods are required to get mechanistic insights into the stability of drug-loaded nanocarriers in biologically relevant media simultaneously avoiding the use of *in vivo* animal models. Indeed, there are currently some research methods available to explore the stability of drug-loaded polymeric micelles in well-defined and simple media, for example, dialysis [30,31] and particle size analysis [32,33]. However, these methods cannot give a clear indication of the stability of nanomedicines in complex biological media such as blood. An attractive technology, and hardly exploited for this purpose, is asymmetrical flow field-flow fractionation (AF4), which allows high resolution separation of particles and plasma proteins based on size differences under physiologically relevant conditions [34].

In the present study, the *in vitro* and *in vivo* stability of mTHPC-loaded dithiolane-crosslinked micelles based on poly(ε-caprolactone)-*co*-poly(1,2-dithiolane-carbonate)-*b*-poly(ethylene glycol) (p(CL-*co*-DTC)-PEG) was investigated. In our previous study, it was shown that p(CL-*co*-DTC)-PEG micelles crosslink spontaneously by disulfide-exchange between dithiolanes in the core of the micelles [35]. Here, the *in vitro* release of mTHPC from these covalently crosslinked p(CL-*co*-DTC)-PEG micelles and the *in vitro* stability of these micelles as well as of non (covalently)-crosslinked pCL-PEG based micelles in human plasma was evaluated by fluorescence spectroscopy and AF4. To validate the *in vitro* findings, the *in vivo* pharmacokinetics including circulation kinetics and tumor accumulation of the crosslinked micelles as well as the loaded mTHPC were studied in A431 tumor-bearing mice and compared with that of free mTHPC and non (covalently)-crosslinked pCL-PEG based micelles loaded with the same PS.

2. Materials and methods

2.1. Materials

Benzyl-poly(ε-caprolactone)-*b*-poly(ethylene glycol) (pCL-PEG) block copolymers with different molecular weights of CL and a fixed molecular weight of PEG of 2 kDa (measured by ^{1}H NMR; Supplementary **Scheme S1A**) were synthesized and characterized as described in our previous publication [17]. Poly(ε-caprolactone)-*co*-poly(1,2-dithiolane-carbonate)-*b*-poly(ethylene glycol) (p(CL-*co*-DTC)-PEG) block copolymers with a random or blocky distribution of CL and DTC in polyester/carbonate blocks (*i.e.,* random p(CL-DTC)-PEG and blocky p(CL-*b*-DTC)-PEG) were synthesized by simultaneous and sequential copolymerization of CL and DTC using methoxy-poly(ethylene glycol) (mPEG-OH, 2 kDa) as initiator (**Scheme S1B**, supporting information), respectively, and the monomer sequences in the resulting block copolymers were analyzed by ^{1}H/^{13}C NMR analysis, as described previously [35]. The characteristics of the synthesized block copolymers are summarized in **Table S1** (Supporting information) and some representative ^{1}H NMR spectra and GPC curves are shown in Figs. S1-S3 (these data have been published before in [17,35], but for the convenience of the reader of the present paper, we report them again here in the supporting information). p(CL-*co*-DTC) oligomers were synthesized as described in **section S1** of the supporting information. Phosphate buffered saline (PBS, pH 7.4, containing 11.9 mM phosphates, 137 mM sodium chloride and 2.7 mM potassium chloride) was obtained from Fischer Bioreagents (Bleiswijk, the Netherlands). Radioimmunoprecipitation assay (RIPA) lysis buffer (10×, 0.5 M Tris-HCl, pH 7.4, 1.5 M NaCl, 2.5% deoxycholic acid, 10% NP-40, 10 mM EDTA) was purchased from Merck KGaA (Darmstadt, Germany). Standard regenerated cellulose dialysis tubing (Spectra/Por®6) with molecular weight cutoff (MWCO) of 1 kDa was purchased from Spectrumlabs (Rancho Dominguez, Califonia, USA). Maleimide functionalized cyanine7 fluorescent dye (Cy7-maleimide) was ordered from Lumiprobe Corporation (Hannover, Germany). 1,4-Dithiothreitol (DTT) was a product of Sigma Aldrich (Zwijndrecht, the Netherlands). m-Tetra(hydroxyphenyl) chlorin (mTHPC) was obtained from Molekula (Munich, Germany). All other solvents and reagents were obtained from Biosolve (Valkenswaard, the Netherlands).

2.2. Synthesis and characterization of Cy7-labeled p(CL-co-DTC)-PEG

Cy7-labeled p(CL_{18}-$DTC_{7.5}$)-PEG block copolymer was synthesized as previously reported [17] (**Scheme S2**, supporting information). The successful coupling of Cy7 to the polymer and complete removal of unreacted Cy7 was demonstrated by GPC analysis, with which the amount of Cy7 in the copolymer was quantified using UV/Vis detection at 755.5 nm, showing 17% coupling efficiency as reported previously [17]. On average, one polymer chain carried ~0.2 Cy7 molecule.

2.3. Preparation and characterization of empty and mTHPC-loaded micelles

Non (covalently)-crosslinked micelles consisting of 10 mg/mL pCL-PEG without and with 0.5 and 5 wt% mTHPC loadings were prepared using a film hydration method, as described previously [16,17]. Covalently crosslinked micelles based on different dithiolane containing p(CL-*co*-DTC)-PEG block copolymers (4 mg/mL polymer) were prepared by a nanoprecipitation method, as previously reported [17,22]. Briefly, for empty micelles, 4 mg copolymer was dissolved in 100 μL of DMF (40 mg/mL), while for mTHPC loaded crosslinked p(CL-*co*-DTC)-PEG micelles (different loadings), a certain volume of mTHPC solution in DMF (5 mg/mL, volume depending on the aimed wt% loading), was added to the weighted polymer, followed by addition of a certain volume of DMF to obtain a final polymer concentration of 40 mg/mL. Subsequently, the resulting copolymer/mTHPC solution was added dropwise to PBS, at 1/9 volume ratio. Homogenous micellar dispersions were formed after gentle shaking and subsequently dialyzing the obtained dispersion using a dialysis tubing (MWCO =1 kDa) against PBS at room temperature for 12 h.

The *Z*-average hydrodynamic diameter (Z_{ave}) and polydispersity index (PDI) of the formed micelles were determined by dynamic light scattering (DLS) using a ZetaSizer Nano S (Malvern). The loading capacity (LC) and loading efficiency (LE) of mTHPC were determined by UV–Vis analysis and calculated using following equations as previously reported [16].

$$LE\ (\%) = \frac{mTHPC\ loaded\ (mg)}{mTHPC\ in\ the\ feed\ (mg)} x100\%$$

$$LC\ (\%) = \frac{mTHPC\ loaded\ (mg)}{polymer\ used\ (mg) + mTHPC\ loaded\ (mg)} x100\%$$

2.4. In vitro stability studies

2.4.1. In vitro release of mTHPC from micelles as studied by fluorescence spectroscopy

The *in vitro* release of mTHPC from (de)crosslinked p(CL-*co*-DTC)-PEG micelles (10 wt% mTHPC loading, prepared in PBS as described in section 2.3) was studied in human plasma (from Seralab, UK) at 37 °C by monitoring the change of fluorescence intensity of mTHPC, as previously reported [16]. Free mTHPC (*i.e.,* mTHPC in a solution of ethanol/propylene glycol (40/60, *w*/w)) was used as reference. In short, 960 μL of mTHPC-loaded crosslinked micelles in PBS (4 mg/mL polymer) were pre-incubated with 80 μL of 20 mg/mL DTT solution in PBS (final DTT concentration was 10 mM) to reduce disulfide bonds in the core of the micelles, or with 80 μL PBS at 37 °C for 12 h as a control. Subsequently, the pretreated micelles as well as free mTHPC were added to human plasma or PBS (as control) at a volume ratio of 1/9. During incubation with plasma at 37 °C, samples were taken at different time points (5 min, and 0.5, 1, 1.5, 2, 3, 5, 8 h) and placed in a 384-well plate to record the fluorescence intensity using a Jasco FP8300 spectrofluorometer (Japan) at 655 nm after excitation at 420 nm.

2.4.2. Stability of empty and mTHPC-loaded micelles as studied by AF4

Asymmetric flow field-flow fractionation (AF4) was used to investigate the *in vitro* stability of empty micelles in human plasma as well as the release of mTHPC from micelles in a solution of human serum albumin (HSA) or human plasma (both from Sigma Aldrich, Darmstadt, Germany). For this purpose, covalently crosslinked p(CL-*co*-DTC)-PEG micelles with random monomer order in the hydrophobic block (4 mg/mL polymer) and non (covalently)-crosslinked pCL-PEG micelles (10 mg/mL polymer) without and with mTHPC loadings (5 and 0.5 wt%) were prepared in PBS as described in section 2.3. In detail, empty micelles were mixed with human plasma or PBS at a volume ratio of 7/3. To study release, mTHPC-loaded micelles were incubated either with HSA solution in PBS (final HSA concentration was 45 mg/mL) or human plasma at a volume ratio of 7/3, while free mTHPC (*i.e.,* mTHPC in a solution of ethanol/propylene glycol (40/60, *w*/w)) at mTHPC concentrations of 0.5 and 0.05 mg/mL (corresponding to the amounts that were present in 5 and 0.5 wt% mTHPC loadings in pCL-PEG micelles) was employed as reference. During incubation at 37 °C, samples were taken at predetermined time points ranging from 0 to 24 h and analyzed by AF4.

AF4 measurements were performed using an AF2000 separation system (Postnova Analytics, Landsberg, Germany) equipped with PN1130 isocratic pumps, degasser and different detectors, namely a refractive index (RI, PN3150) detector, a fluorescence (PN3412) detector and a DLS (Zetasizer Nano ZS, Malvern Instruments, Herrenberg, Germany**)** detector, respectively. The separation channel consisted of a spacer with 350 μm thickness, deltoid shaped channel profile and 27 cm channel length, and a regenerated cellulose membrane with a cut-off of 10 kDa from Postnova Analytics (Landsberg, Germany). PBS was used as a mobile phase.

A 50 μL of sample was injected into the system during the focusing step with an injection flow rate of 0.2 mL/min, and a focus flow rate of 3 mL/min over 4 min. Next, in the fractionation step, after a transition time of 1 min, the crossflow was kept constant at 2.7 mL/min for 7 min and then decreased exponentially in 20 min to 0.1 mL/min. The crossflow was kept constant at 0.1 mL/min for 15 min and at 0.00 mL/min for another 4 min to ensure complete sample elution. Samples were eluted with a flow rate of 0.5 mL/min. Detailed flow rates in each step and mechanism of AF4 are presented in **Table S3**, **Section S2** and **Scheme S3** (supporting information), respectively. The detection of the eluted and fractionated protein components and (mTHPC loaded) micelles was performed sequentially by RI, fluorescence at λ_{em} 650 nm with λ_{ex} 420 nm (for mTHPC) and DLS. The AF2000 control unit software was used for data acquisition and processing.

2.5. In vivo studies of free mTHPC and Cy7 labeled micelles loaded with mTHPC in A431 tumor-bearing mice

For the *in vivo* studies, mTHPC (0.6 wt% loading) in dithiolane-crosslinked p(CL_{18}-$DTC_{7.5}$)-PEG micelles with random monomer order in the hydrophobic block and non (covalently)-crosslinked pCL_{23}-PEG micelles were prepared in PBS as described in section 2.3, except that the micelles were labeled by mixing the corresponding non-labeled polymers with Cy7-labeled p(CL_{18}-$DTC_{7.5}$)-PEG (synthesis is described in section 2.2) (at a ratio of 98.5 to 1.5% *w*/w) before preparation of the micelles. mTHPC injection solution was prepared by 1:1 dilution of a 120 μg/mL mTHPC stock solution in solvent (*i.e.,* ethanol/propylene glycol, 40/60 w/w) with PBS (final mTHPC concentration was 60 μg/mL, equal to the concentration of injected micellar samples with 0.6 wt % mTHPC loading).

The animal experiments were approved by the local Utrecht animal ethics welfare committee and national regulatory authorities. Female Balb/c nude mice, weighing 20–28 g were purchased from Envigo (Horst, the Netherlands). Mice were housed in ventilated cages at 25 °C and 55% humidity under natural light/dark conditions. Food and water were provided *ad libitum* during the entire study. Mice were inoculated with 1×10^6 A431 cells suspended in 100 μL PBS subcutaneously into the right flank. When the tumors reached a size of 100–300 mm^3, mice were included in the studies. Tumors were measured using a digital caliper. The tumor volume V (in mm^3) was calculated using the eq. $V = (\pi/6)LS^2$ where L is the largest and S is the smallest superficial diameter [19].

2.5.1. Circulation kinetics

Two groups of tumor-bearing mice (n = 3–6 per group) were intravenously (*i.v.*) injected *via* the tail vein with free mTHPC dissolved in ethanol/propylene glycol/PBS (20/30/50, *v*/v/v) or mTHPC-loaded Cy7-labeled p(CL_{18}-$DTC_{7.5}$)-PEG micelles, respectively, at injection doses of 300 μg mTHPC/kg, corresponding to a dose of ~6 μg mTHPC per mouse.

Blood samples were collected in tubes with EDTA-anticoagulant *via* submandibular puncture (~60 μL) at 1 min (100% injection control), and at 1 and 2 h, and *via* cardiac puncture (~200 μL) after 4 and 24 h, post injection. For the latter, mice were killed through cervical dislocation while under deep isoflurane anesthesia. The collected blood samples were centrifuged at 1000 ×*g* for 15 min at 4 °C. The plasma supernatant was collected, extracted using acetonitrile/DMSO (4/1, *v*/v) and analyzed by high-performance liquid chromatography (HPLC) and a LI-COR Odyssey imaging system to quantify the amount of mTHPC and Cy7 labeled polymer, respectively, as described in previous papers [17,22]. Pharmacokinetic parameters were determined by non-compartmental analysis with the PKSolver add-in for Microsoft Excel [36].

2.5.2. Biodistribution in tumor-bearing mice

Mice were sacrificed 4 and 24 h (3–6 animals per group) after *i.v.* administration of the formulations including free mTHPC and mTHPC-loaded Cy7-labeled covalently crosslinked p(CL_{18}-$DTC_{7.5}$)-PEG and non (covalently)-crosslinked pCL_{23}-PEG micelles. Tumors were excised and then stored at −80 °C until further processing for quantification. Tumors from three untreated animals were used as controls.

To quantify the content of mTHPC and Cy7 labeled micelles in the tumors, the excised tumor samples were treated [22]. In short, to weighted tumor samples, an equal volume of RIPA lysis buffer (*v*/*w*) was added. The mixture was homogenized at a speed of 6000/s for 60 s and the homogenate was subsequently aliquoted.

To determine the mTHPC concentration in the samples, an aliquot of the homogenate was vortex-mixed with acetonitrile/DMSO (4/1 *v*/v) at a volume ratio of 1 to 4 for 1 min. After centrifugation at 15,000 ×*g* for

10 min, 50 μL of the obtained supernatant was injected into the HPLC system consisting of a Waters X Select CSH C18 3.5 μm 4.6 × 150 mm column coupled with a fluorescence detector set at λ_{ex} 420 nm, λ_{em} 650 nm to analyze the mTHPC concentrations in the different samples [22]. To determine the concentration of Cy7 labeled micelles, another aliquot of the homogenate was vortex-mixed with RIPA lysis buffer (1/2, *v*/v) for 1 min. The fluorescence of Cy7 in the mixture (20 μL) was detected at the 800 nm channel (*i.e.* λ_{ex} 785 nm and λ_{em} 820 nm), using a LI-COR Odyssey scanner imaging system [22].

2.6. Statistical analysis

Statistical analysis was done by GraphPad Prism 8.3.0 software. Statistical significance of biodistribution among different mTHPC formulations was determined by two-way analysis of variance (ANOVA). A value of $p < 0.05$ was considered significant. Statistical significance is depicted as * p ˂ 0.05, ** p ˂ 0.01, *** p ˂ 0.001.

3. Results and discussion

3.1. Preparation and characterization of polymeric micelles

Spontaneously crosslinked micelles based on dithiolane (p(CL-*co*-DTC)-PEG) at a polymer concentration of 4 mg/mL were prepared by a previously reported nanoprecipitation method [17,22]. Non (covalently)-crosslinked micelles consisting of 10 mg/mL pCL-PEG were prepared by a film hydration method [16,17]. Different block copolymers were chosen for the preparation of crosslinked micelles, which differed in the sequence of CL and DTC (*i.e.*, blocky or random) and/or molecular weight of the hydrophobic block (**Table S1**, supporting information). As reported previously and summarized in **Fig. S4** (supporting information) [35], the covalently crosslinked p(CL-*co*-DTC)-PEG micelles had hydrodynamic diameters that slightly increased from 17 to 22 nm with increasing chain length of the hydrophobic block from ~12 to ~25 monomeric units, independent of the monomer sequence (*i.e.*, blocky or random distribution of CL and DTC in the polymer chain). In contrast, for non (covalently)-crosslinked pCL-PEG micelles, the increase in sizes was more significant (from 17 to 43 nm), with increasing CL chain length from 9 to 23 units (**Fig. S4**, supporting information) [17] which can probably be explained by the more condensed p(CL-*co*-DTC)-PEG micellar core caused by crosslinking compared to the non (covalently)-crosslinked pCL-PEG micelles. At least, the sizes measured by DLS of non (covalently)-crosslinked pCL-PEG micelles were well in agreement with that obtained by TEM measurements [37]. The different micelles were able to efficiently load mTHPC (~80%) in the micellar core at mTHPC feed concentration of ~0.5 mg/mL, which is in line with our previously published data [16,17].

3.2. In vitro stability studies

3.2.1. In vitro release of mTHPC from micelles in human plasma as studied by fluorescence spectroscopy

The *in vitro* release of mTHPC from the crosslinked p(CL-*co*-DTC)-PEG micelles was investigated in human plasma over time at 37 °C (Fig. 1), by making use of the quenched state when mTHPC is aggregating in the core of the micelles and fluorescence dequenching that occurs after its release from the micelles [16]. To explain, when mTHPC releases from the micelles, fluorescence intensity increases resulting from a combination of fluorescent mTHPC when it is released and simultaneous less fluorescence quenching of retained PS in the core of the micelles. Similar as observed in our previous study [16], when free mTHPC (dissolved in a mixture of ethanol and propylene glycol) was added to PBS, severe precipitation occurred and hardly any fluorescence was detected (**Fig. S5A**, black line, supporting information). Upon 10× dilution of micelles in PBS, the fluorescence of mTHPC when loaded in the micelles was quite low and constant over 8 h at 37 °C due to the afore-mentioned fluorescence quenching (**Fig. S5A**, supporting information). However, upon 10× dilution in plasma, free mTHPC showed fluorescence intensity of ~2100 a.u. (Fig. 1, black lines), indicating the capability of plasma proteins to solubilize mTHPC. For mTHPC loaded in crosslinked micelles consisting of p(CL-*co*-DTC)-PEG with relatively short chain lengths of the hydrophobic blocks (9 units of CL and 4 to 7 units of DTC) (Fig. 1A, red, green and cyan lines), substantial increase of fluorescence was observed during the first 1 h incubation with plasma. This figure also shows that the fluorescence intensities levelled off at ~2100 a.u., identical to fluorescence intensity observed from free mTHPC (black line), suggesting complete and quite rapid release of mTHPC from these micelles in plasma. This was observed regardless of the monomer sequence and the DTC content in the polymer chains, and was consistent with our previous studies on non (covalently)-crosslinked pCL_9-PEG and $pCL_{17.6}$-PEG based micelles having similar short hydrophobic pCL blocks [16,22]. However, for the crosslinked p(CL_{18}-$DTC_{7.5}$)-PEG micelles containing longer hydrophobic block (Fig. 1A, pink line, ~25 units of CL and DTC in total), quantitative release of mTHPC from the micelles took longer (~4 h), suggesting better mTHPC retention in these micelles. In our previous study, we also demonstrated that increasing the pCL hydrophobic block from 9 to 23 units resulted in better retention of mTHPC (0.5 and 8 h, respectively) [17]. Therefore, as compared to micelles with shorter hydrophobic blocks, the slower release of mTHPC from p(CL_{18}-$DTC_{7.5}$)-PEG micelles can be explained by the chemical crosslinking and/or the increased hydrophobic interactions, both responsible for stabilization of micelles [38,39]. Interestingly, despite more or less similar chain lengths of the core-forming hydrophobic blocks, the slower release of mTHPC from the non (covalently)-crosslinked pCL_{23}-PEG micelles as compared to the covalently crosslinked ones (8 *vs* 4 h) might be ascribed to the physical state of the

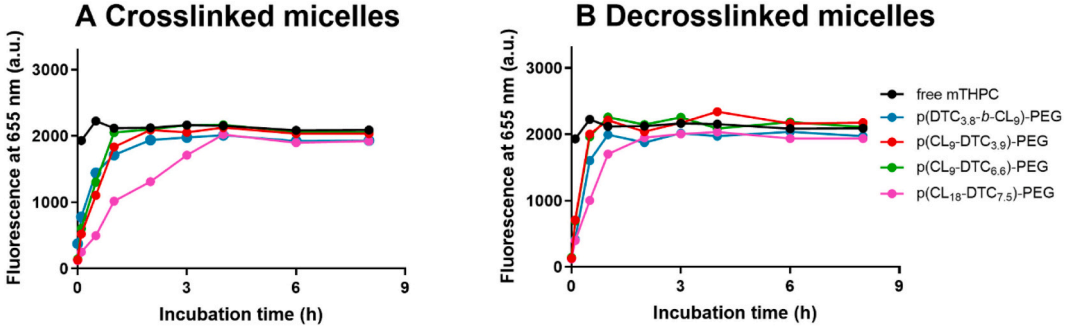

Fig. 1. Fluorescence intensity (λ_{ex} 420 nm, λ_{em} 655 nm) of free mTHPC and mTHPC-loaded (10 wt%) (de)crosslinked p(CL-*co*-DTC)-PEG micelles as a function of time at 37 °C in human plasma; free mTHPC and micelles were 10× diluted with human plasma to obtain final polymer and mTHPC concentrations of 0.4 mg/mL and 32 μg/mL, respectively. The fluorescence intensities of the corresponding mTHPC-loaded micelles diluted with PBS were used as 0 h timepoint. Decrosslinked micelles were prepared by incubation of their crosslinked counterparts with DTT (10 mM in PBS, to reduce the disulfide bonds) for 12 h at 37 °C.

core-forming hydrophobic blocks at 37 °C, as a result of the different melting points of pCL_{23} and $p(CL_{18}\text{-}DTC_{7.5})$ hydrophobic blocks (T_m: 45 *vs* 20 °C with ΔH_m: 86 *vs* 21 J/g, **Table S2** in supporting information). In other words, the semi-crystalline state with crystallites acting as physical crosslinks in the core-forming hydrophobic pCL block in the pCL_{23}-PEG micelles may confer greater PS retention by decreasing its rate of diffusion [39–41] as compared to the liquid state of the core of $p(CL_{18}\text{-}DTC_{7.5})$-PEG micelles at 37 °C.

After reduction by DTT of the disulfide bonds present in the core of the p(CL-*co*-DTC)-PEG based micelles (*i.e.,* decrosslinking) and subsequent incubation in plasma, faster increase in the fluorescence intensity of mTHPC was observed (Fig. 1B) compared to the micelles before decrosslinking (Fig. 1A), *i.e.*, the plateau fluorescence reached within 1 h. This observation demonstrates that a faster release of mTHPC from micelles can be triggered by reversible reduction of disulfide bonds present in the micellar core resulting in decrosslinking of the micelles.

3.2.2. Stability of empty and mTHPC-loaded micelles as studied by AF4

3.2.2.1. Stability of empty micelles in human plasma. AF4 as a fractionation technique provides opportunities to separate particles and proteins in complex mixtures based on their hydrodynamic sizes [34]. Therefore, this technique was exploited to assess whether micellar disassembly resulting from protein-micelle interactions plays a role in the mTHPC release profiles shown in section 3.2.1. To this end, empty covalently crosslinked $p(CL_9\text{-}DTC_{3.9})$-PEG and $p(CL_{18}\text{-}DTC_{7.5})$-PEG micelles and non (covalently)-crosslinked pCL-PEG micelles that showed different retention characteristics of mTHPC in the presence of plasma (as discussed in section 3.2.1) were incubated with plasma at 37 °C and subsequently fractionated and analyzed using AF4.

Fractograms obtained by refractive index (RI) detection of the empty micelles in PBS at 37 °C did not change upon 24 h incubation, regardless of being covalently crosslinked or not and of their initial sizes (**Fig. S6**, supporting information), demonstrating excellent stability of the

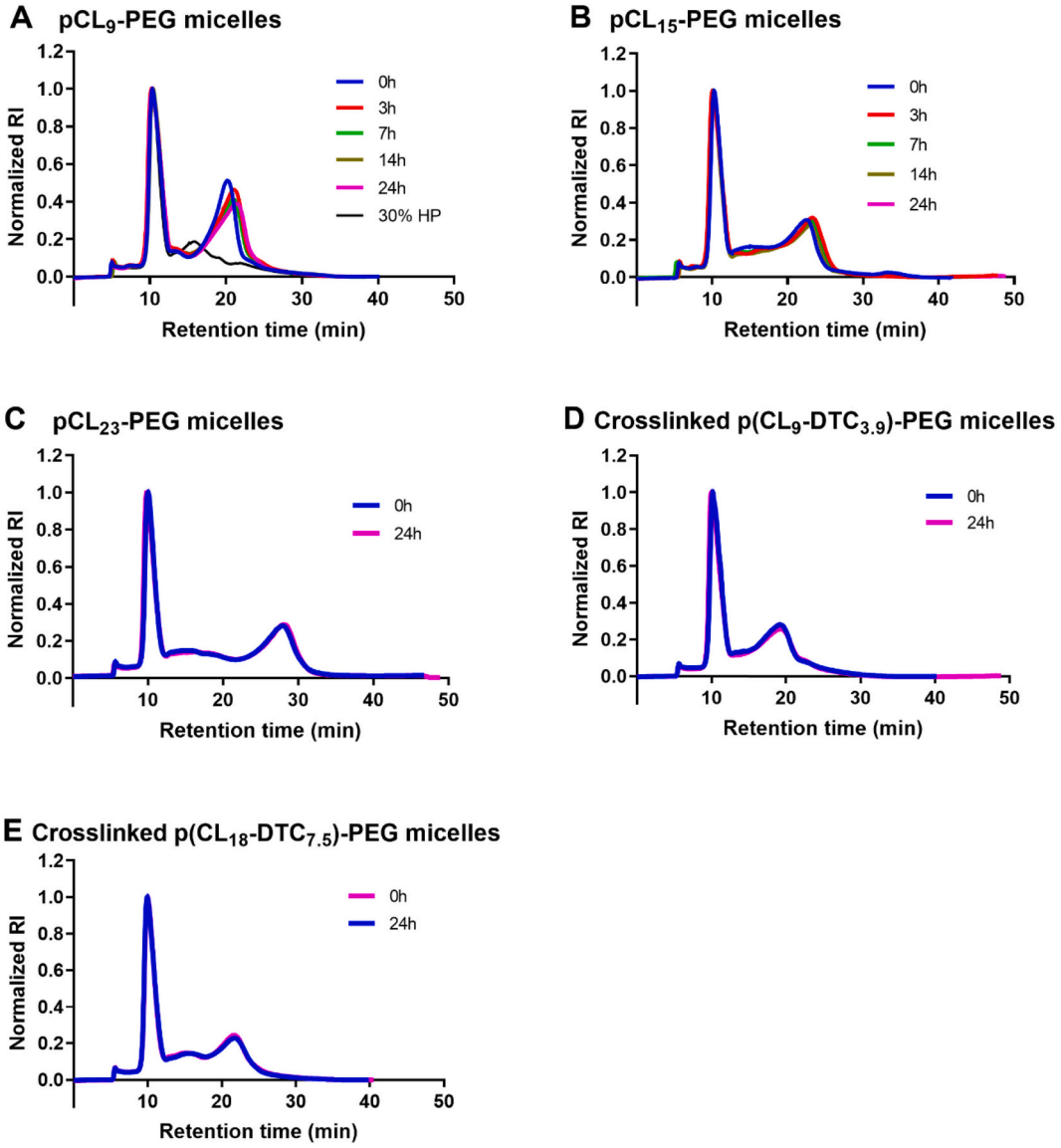

Fig. 2. AF4 fractograms of micelles using refractive index (RI) detection. The micelles were incubated for 24 h with human plasma (HP) at 37 °C: non (covalently)-crosslinked micelles composed of pCL_9-PEG (A), pCL_{15}-PEG (B) and pCL_{23}-PEG (C) and dithiolane crosslinked micelles consisting of $p(CL_9\text{-}DTC_{3.9})$-PEG (D) and $p(CL_{18}\text{-}DTC_{7.5})$-PEG (E) were incubated with plasma at a volume ratio of 7/3 for 24 h. After being mixed with plasma, the final polymer concentrations of non (covalently)-crosslinked pCL-PEG and crosslinked p(CL-*co*-DTC)-PEG based micelles were 7.0 and 2.8 mg/mL, respectively. A sample of human plasma (donated as 30% HP in (A)) was used to assign the peaks of plasma components. The signals were normalized to the highest signal.

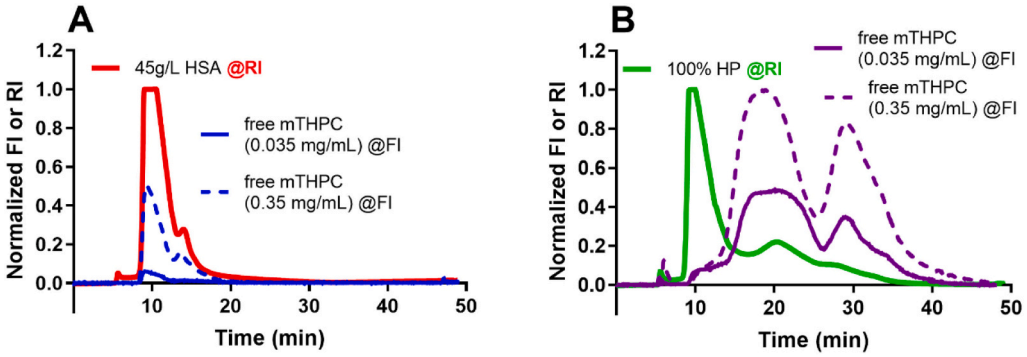

Fig. 3. Fractograms of free mTHPC in PBS with 45 g/L HSA (A) and 100% human plasma (B) obtained by refractive index (RI) (A, red line and B, green line) and fluorescence intensity (FI) (λ_{ex} 420 nm, λ_{em} 650 nm) (A, blue lines and B, purple lines); free mTHPC was added at a final concentration of 0.035 and 0.35 mg/mL, respectively. The signals were normalized to the highest signals. (For interpretation of the references to colour in this figure legend, the reader is referred to the web version of this article.)

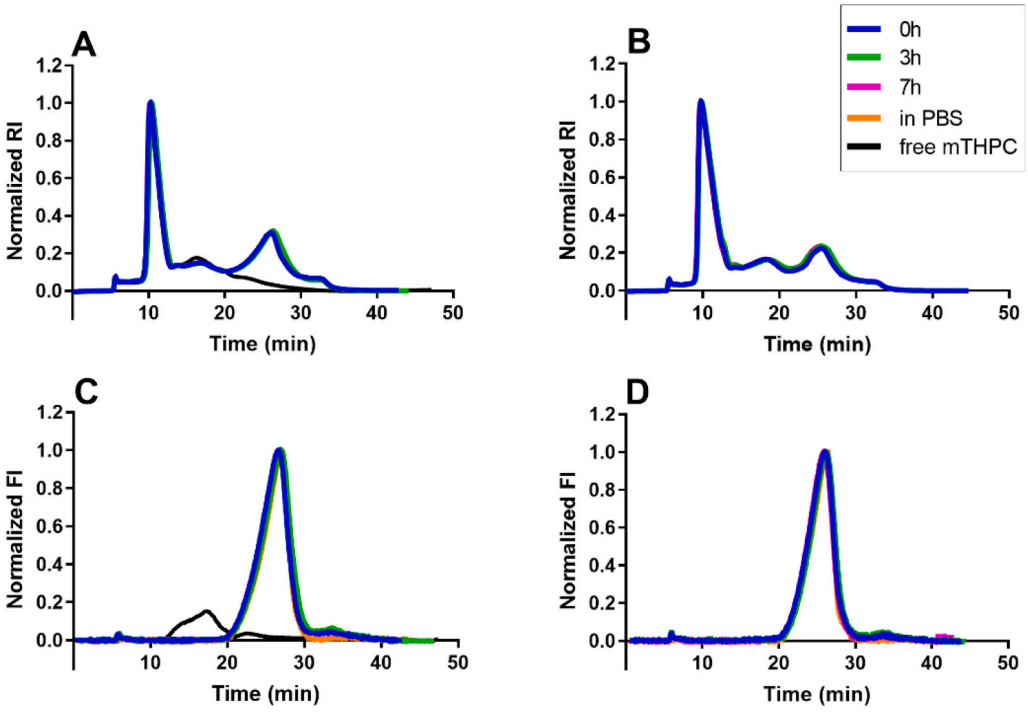

Fig. 4. Fractograms of mTHPC-loaded (0.5 wt%) pCL_{23}-PEG micelles incubated for 7 h with human plasma (HP) at 37 °C and at PBS/plasma volume ratios of 7/3 (A, C) and 4/6 (B, D), respectively, obtained by refractive index (RI) (A, B) and fluorescence intensity (FI) (λ_{ex} 420 nm, λ_{em} 650 nm) (C, D). After being mixed with plasma, the final polymer concentrations were 7 (A, C) and 4 (B, D) mg/mL, respectively. As a control, free mTHPC at a final concentration of 0.035 mg/mL was added to plasma (black line), corresponding with the concentrations obtained from micelles with 0.5 wt% mTHPC loadings. The signals were normalized to the highest signals.

micelles in PBS. In line with this, the size distribution of these micelles as measured by in-line DLS did not change over 24 h in PBS (**Fig. S7**, supporting information). When the different micelles were incubated with plasma, two well-separated main peaks were observed (Fig. 2), namely one at retention time of ~10 min, representing human serum albumin (as verified by overlaying the fractograms with that of human plasma, *e.g.,* Fig. 2A, blue *vs* black line) and another at retention times ranging from approximately 20 to 30 min, corresponding to micelles (as evidenced by the fractograms of micelles in PBS, **Fig. S6**, supporting information). In-line DLS measurements of the micelles in plasma (**Fig. S8**, supporting information) showed an increase in particle size with increasing retention time, as expected, which did not significantly change over the course of the 24 h incubation time. However, it is clear (**Fig. 2A** and **B)** that the peak corresponding to both non-(covalently)-crosslinked pCL_9-PEG and pCL_{15}-PEG micelles with relatively small sizes (<25 nm) shifted to higher retention times and thus increased in size with increasing incubation time, suggesting a certain degree of instability of these micelles. Probably, the observed release of mTHPC from the pCL_9-PEG and $pCL_{17.6}$-PEG micelles in plasma as described in our previous publications [16,22] is related to the instability of these micelles as shown by the AF4 data. Interestingly, shifts of the micellar peaks were not observed for the covalently crosslinked p(CL_9-$DTC_{3.9}$)-PEG and p(CL_{18}-$DTC_{7.5}$)-PEG micelles with similar relatively small sizes (<25 nm) (**Fig. 2D** and **E**), as well as for the physically crosslinked pCL_{23}-PEG micelles (Fig. 2C) with a larger size (43 nm), suggesting that these micelles were stable in this medium.

From above data, we can draw several conclusions. First, it is noted that covalently crosslinked p(CL_9-$DTC_{3.9}$)-PEG micelles showed superior stability in plasma, as compared to the non (covalently)-crosslinked pCL_9-PEG micelles of similar size (18 *vs* 17 nm) and pCL_{15}-PEG micelles that have comparable chain length of the hydrophobic segment (~14 monomer units) but slightly differed in size (~18 *vs* ~ 24 nm). This indicates that indeed covalent-crosslinking improves the stability of small micelles in plasma. Likewise, covalently crosslinked p(CL_{18}-$DTC_{7.5}$)-PEG micelles had better stability as compared to non (covalently)-crosslinked pCL_{15}-PEG micelles having comparable sizes (22 *vs* 24 nm). On the other hand, non (covalently)-crosslinked pCL_{23}-PEG micelles displayed similar high stability when compared to p(CL_{18}-$DTC_{7.5}$)-PEG micelles, which have similar chain lengths (~24 monomer units) of the core-forming block but different sizes (43 *vs* 22 nm). As discussed in section 3.2.1, this is probably attributed to physical crosslinks resulting from the crystallization of pCL blocks in the core of the

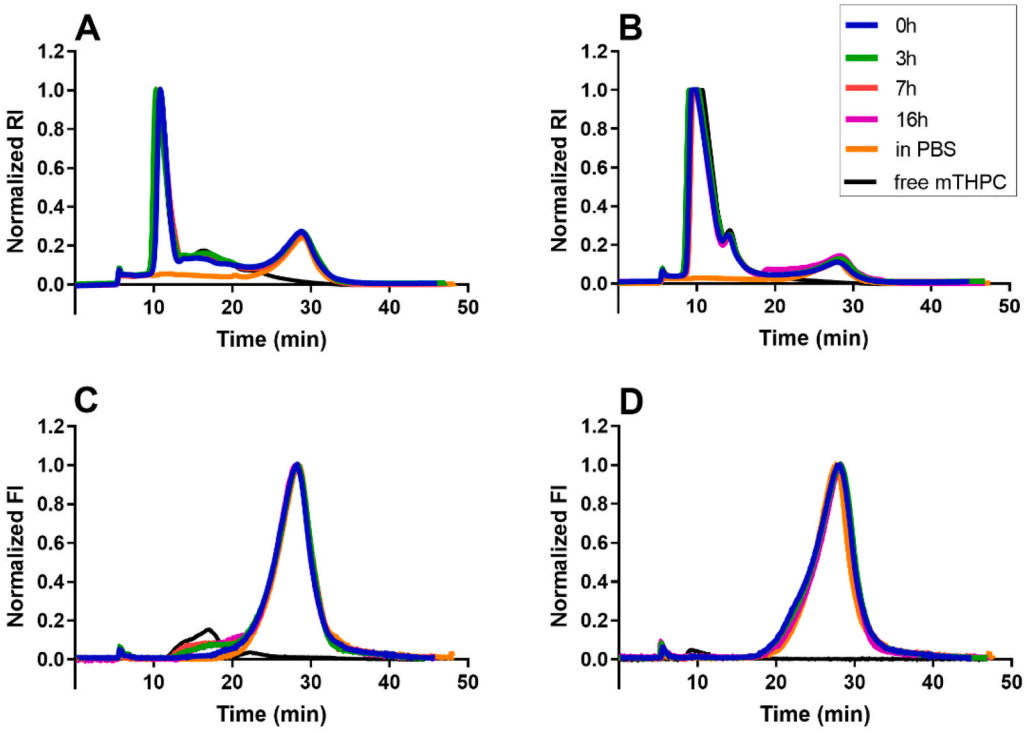

Fig. 5. Fractograms of mTHPC-loaded (5 wt%) pCL_{23}-PEG micelles incubated at 37 °C for 16 h with plasma (7/3, *v*/v) (A, C) or 45 g/L HSA (B, D), obtained by refractive index (RI) (A, B) and fluorescence intensity detection (FI) (λ_{ex} 420 nm, λ_{em} 650 nm) (C, D). After being mixed with plasma or HSA (solution in PBS), the final polymer concentrations of the different micelles were 7.0 mg/mL. As a control, free mTHPC at a final concentration of 0.035 mg/mL was added to plasma and HSA, corresponding to the same concentration of mTHPC in 0.5 %wt loading in the micelles. The signals were normalized to the highest signals (RI or FI).

pCL_{23}-PEG micelles (so these micelles are referred to physically crosslinked pCL_{23}-PEG micelles from here). In fact, according to the obtained AF4 results for the non (covalently)-crosslinked pCL-PEG micelles, the stability of these micelles improved by increasing the chain length of hydrophobic pCL block from 9 to 23 units (see Figs. 2A-C).

3.2.2.2. Release of mTHPC from micelles in buffer with human serum albumin and human plasma as studied by AF4. Besides protein-polymer interactions, favorable interactions of the loaded cargo with plasma proteins can also lead to its premature release from the micelles, even when the nanoparticles are stable in plasma [42–44]. Previous studies showed high binding affinity of mTHPC for plasma (lipo)proteins leading to mTHPC redistribution from intact liposomes to lipoproteins [26–29]. Indeed, we also observed that even though the empty covalently crosslinked p(CL_9-$DTC_{3.9}$)-PEG and p(CL_{18}-$DTC_{7.5}$)-PEG micelles are stable in plasma for 24 h according to the AF4 data shown above, mTHPC was quantitatively released from these micelles in 1 and 4 h, respectively (see Fig. 1A, red and pink lines). To investigate this further, mTHPC loaded in stable micelles (*i.e.,* covalently crosslinked p(CL_9-$DTC_{3.9}$)-PEG and p(CL_{18}-$DTC_{7.5}$)-PEG micelles or physically crosslinked pCL_{23}-PEG micelles) with different mTHPC loadings, were incubated with human serum albumin (HSA) or human plasma for 16 h at 37 °C. RI detection was used to record fractograms of plasma components and micelles, while mTHPC was also detected making use of its intrinsic fluorescence using a fluorescence detector coupled to the AF4.

By comparing the RI fractograms of HSA (Fig. 3A, red line) and plasma (Fig. 3B, green line), it can be concluded that the peak of plasma at approximate 10 min represents the most abundant component, *i.e.,* albumin, whereas the broad peak at around 20 and 30 min corresponds to low- and high-density lipoproteins, respectively. Importantly, it is obvious from Fig. 3B (purple lines) that free mTHPC preferably binds to lipoproteins, particularly low-density lipoproteins which is in agreement with previous studies [29,45], while in the absence of lipoproteins it just slightly binds to albumin (Fig. 3A, blue lines).

For mTHPC-loaded pCL_{23}-PEG micelles, fractograms obtained by RI detection show that the peak of the micelles (retention time of ~30 min.) did not change upon incubation regardless of the medium (HSA or plasma) (0.5 wt% loading, **Fig. 4A**, **B** and 5 wt% loading, Fig. 5A, B), which is in line with the stability results of the corresponding empty micelles (Fig. 2C). The fractograms obtained by recording the intrinsic fluorescence of mTHPC (**Fig. 4C** and **D**) after 7 h incubation with either 30 or 60% plasma show no detectable release of mTHPC from pCL_{23}-PEG micelles with 0.5 wt% loading. This suggests good mTHPC retention in pCL_{23}-PEG micelles, which is in good agreement with the release profile based on the quenching of mTHPC fluorescence reported in our previous study [17]. On the other hand, upon incubation with 30% plasma of pCL_{23}-PEG micelles with 5 wt% mTHPC loading, a small fluorescence peak at approximately 15 min in the fractogram (Fig. 5C) was observed after 3 h and did not change till 16 h, suggesting that initially a small fraction (< 5%) of mTHPC was released and subsequently bound to lipoproteins probably as a result of overloading of the core of the micelles with mTHPC. In contrast, the release of mTHPC in HSA was negligible (Fig. 5D), which demonstrates that the release of this PS from pCL_{23}-PEG micelles is medium dependent and emphasizes the high affinity of the PS for lipoproteins and not for albumin.

The release of mTHPC from covalently crosslinked p(CL-*co*-DTC)-PEG micelles could not be evaluated by AF4 because released mTHPC that bound to lipoproteins has the same retention time as the micelles (~17 min).

Overall, the results of AF4 analysis indicate that this technique is a powerful analytical tool to evaluate the stability of PS loaded micelles in biological media, *e.g.,* blood plasma. It can separate the micelles and different plasma proteins, which is necessary for analysis of possible interactions between proteins and particles but challenging using conventional separation methods, *e.g.,* size exclusion chromatography or ultracentrifugation. In addition, PS (re)distribution to specific plasma proteins is observed, giving strong indications for the (in)stability of PS loaded micelles in plasma. This information is important to explain or even predict micelles' behavior *in vivo* and importantly, provides a valuable reference to take effective measures to prevent possible and unwanted premature cargo release in the circulation.

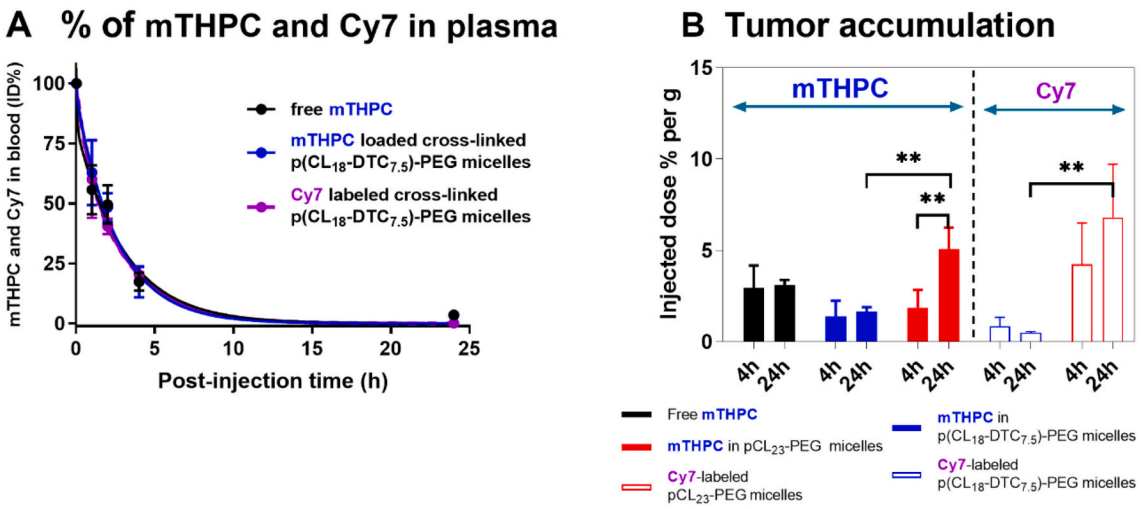

Fig. 6. (A) Circulation kinetics of free mTHPC and mTHPC-loaded (0.6 wt%) Cy7-labeled covalently crosslinked p(CL_{18}-$DTC_{7.5}$)-PEG micelles, showing mTHPC levels (black and blue lines) and Cy7 level (purple line) (B) Biodistribution of free mTHPC and mTHPC-loaded (0.6 wt%) Cy7-labeled p(CL_{18}-$DTC_{7.5}$)-PEG and pCL_{23}-PEG micelles in tumors of mice 4 and 24 h post administration. Data are reported as % of injected doses (ID) upon tail vein administration in A431 tumor-bearing Balb/c mice (300 μg mTHPC/kg, *i.e.* ~6 μg mTHPC/mouse). Data are presented as mean ± SD, $n = 3–5$. (For interpretation of the references to colour in this figure legend, the reader is referred to the web version of this article.)

Table 1
Pharmacokinetic parameters of mTHPC in different formulations and the corresponding (Cy7 labeled) micelles.

Detection	Formulations	Half-life (h)		AUC (h*%)	Volume of distribution (mL/kg)	Clearance (mL/kg/h)
		Phase α[a]	**Phase β**			
mTHPC	Free mTHPC	<0.5	2.1	442	120	13.2
	mTHPC in p(CL_{18}-$DTC_{7.5}$)-PEG micelles	<0.5	2.1	441	116	13.2
	mTHPC in pCL_{23}-PEG micelles	0.7[b]	14.1[b]	928[b]	88[c]	4.6[c]
Cy7	p(CL_{18}-$DTC_{7.5}$)-PEG micelles	<0.5	2.1	397	60	14.7
	pCL_{23}-PEG micelles	0.5[b]	18.1[b]	739[b]	125[c]	4.9[c]

[a] Initial phase half-lives (t½-α) were estimated from plasma disappearance rates during the first hour after administration while half-lives of the terminal phase (t½-β) were calculated from non-compartmental analysis. Distribution volumes and clearances were calculated assuming a standard plasma volume of 58.5 mL/kg [16].
[b] Taken from reference [17].
[c] Calculated from the plasma concentration curves reported in reference [17].

3.3. Circulation kinetics and biodistribution of free mTHPC and Cy7-labeled micelles loaded with mTHPC

In our previous study, we showed and discussed the pharmacokinetics of mTHPC-loaded Cy7-labeled physically crosslinked pCL_{23}-PEG micelles and *i.v.* injected free mTHPC as control [17]. In the present study, the pharmacokinetic data of Cy7-labeled dithiolane-crosslinked p(CL_{18}-$DTC_{7.5}$)-PEG micelles loaded with mTHPC and injected in A431 tumor-bearing mice are reported and discussed, and compared with free mTHPC. Micelles based on p(CL_{18}-$DTC_{7.5}$)-PEG were selected because of the high *in vitro* stability of these empty micelles in plasma (see Fig. 2E) and relatively slow release of mTHPC (see Fig. 1A, pink line). It is noted that no (short term) side effects were observed in mice that received mTHPC-loaded crosslinked p(CL_{18}-$DTC_{7.5}$)-PEG micelles during or after their administration, similar to other pCL-PEG based micelles [17,22].

As indicated in Fig. 6A, the plasma concentration curves of mTHPC after administration of either free mTHPC or the micellar formulation (black and blue lines) were comparable, which is similar to the Cy7 labeled micelles (purple line). It is shown that ~45% of the injected dose (ID) of mTHPC and Cy7 was rapidly cleared in the initial α-elimination phase (first 1 h). Non-compartmental analysis of the mTHPC and Cy7 curves was used to determine pharmacokinetic parameters including terminal half-lives (t½-β), area under the curves (AUCs), distribution volumes and clearances (Table 1). Pharmacokinetic parameters calculated from mTHPC analysis (Table 1, top part) were tightly associated with those derived from Cy7 analysis (Table 1, bottom part). It is however not possible to conclude whether these parameters of mTHPC calculated for the micellar formulation reflect (released) free mTHPC or that remaining associated with the micelles because of coincidently similar data observed for free mTHPC and Cy7. However, combined with the *in vitro* release study (Fig. 1A, pink line), premature release of mTHPC from micelles most likely occurred in the circulation, which was observed in various liposomal mTHPC formulations and other mTHPC-loaded micelles [16,17,46].

Interestingly, the circulation kinetics of pCL_{23}-PEG micelles and mTHPC loaded in those physically crosslinked micelles as well as the corresponding pharmacokinetic parameters presented in [17], were significantly superior as compared to the covalently crosslinked p(CL_{18}-$DTC_{7.5}$)-PEG micelles (Table 1). For instance, we demonstrated that after *i.v.* injection, the PS loaded in pCL_{23}-PEG micelles displayed markedly prolonged blood circulation time (t½-β:14 h), compared to free mTHPC, which is due to the long circulating pCL_{23}-PEG micelles (t½-β:18 h) (Table 1). These results are very well in line with the *in vitro* stability presented in section 3.2 (**Figs. 4 and 5**) and our previous publication [17], which both showed sufficient mTHPC retention in pCL_{23}-PEG micelles during 8 h in human plasma and again indicates that physical crosslinks resulting from the crystallization of pCL blocks in pCL_{23}-PEG micelles confer greater PS retention compared to covalently crosslinks in p(CL_{18}-$DTC_{7.5}$)-PEG micelles.

Finally, the biodistribution of mTHPC loaded in covalently crosslinked p(CL_{18}-$DTC_{7.5}$)-PEG (that showed short circulation time and poor PS retention) and physically crosslinked pCL_{23}-PEG micelles (that had

prolonged circulation time and good PS retention) was investigated and compared with free mTHPC in tumor-bearing mice.

Tumors were excised from mice that were sacrificed at 4 and 24 h post *i.v.* injection of the formulations, and tumor accumulation of Cy7-labeled micelles was quantified by fluorescence intensity measurements (Fig. 6B, open bars). It was shown that Cy7 levels from covalently crosslinked p(CL_{18}-$DTC_{7.5}$)-PEG micelles in tumors were quite low (< 1% ID/g) and remained constant at 24 h (Fig. 6B, open blue bars). Interestingly, tumor accumulation of physically crosslinked pCL_{23}-PEG micelles was much higher than that of covalently crosslinked p(CL_{18}-$DTC_{7.5}$)-PEG micelles (5% *vs* < 1% ID/g) at 4 h and importantly, progressively increased to ~8% upon 24 h after administration (Fig. 6B, open red bars), which led to a significant difference with the crosslinked p(CL_{18}-$DTC_{7.5}$)-PEG micelles. This result demonstrates that long circulating micelles are indeed favorable for EPR-mediated tumor accumulation [18,20,47].

Fig. 6B (solid bars on the left side) displays the biodistribution in tumors of mTHPC that was injected in free form and as covalently crosslinked p(CL_{18}-$DTC_{7.5}$)-PEG or physically crosslinked pCL_{23}-PEG formulations. For free mTHPC and mTHPC loaded in covalently crosslinked p(CL_{18}-$DTC_{7.5}$)-PEG micelles, the mTHPC accumulation in the tumors was similar for 4 and 24 h (~2–3% ID/g) (Fig. 6B, solid black and blue bars). These mTHPC levels were actually higher than Cy7 levels (Fig. 6B, open blue bars), suggesting that mTHPC was not retained within the micelles, *i.e.,* mTHPC was rapidly released from the micelles, in line with the *in vitro* release study (Fig. 1A, pink line). However, when loaded in physically crosslinked pCL_{23}-PEG micelles, the tumor accumulation of mTHPC increased progressively in time (1.8 at 4 h to 5.1% ID/g at 24 h) (Fig. 6B, solid red bars). Despite relatively lower mTHPC level as compared to Cy7 level at each timepoint, this upward trend was correlated well with the Cy7 accumulation in the tumor, demonstrating the ability of long circulating polymeric micelles to facilitate PS targeting to tumors *via* the EPR effect [18,20,47].

4. Conclusion

In the present study, we demonstrated that AF4 is a powerful analytical technique for the separation and characterization of (drug loaded) nanoparticles and its stability in complex biological media *e.g.,* human plasma. PS (re)distribution to lipoproteins was observed, giving strong indications for the (in)stability of the drug-loaded micelles in plasma. With this tool, the (in)stability of drug loaded nanoparticles after *i.v.* administration could be predicted, which is favorable to screen promising delivery systems with reduced experimental time and costs and without excessive use of animals.

Acknowledgement

The research leading to these results resulted from access to the Nanobiotechnology Laboratory under the Framework for open access to the Joint Research Centre Research Infrastructures of the European Commission. Y. Liu is supported by a PhD scholarship from China Scholarship Council (CSC).

Appendix A. Supplementary data

Supplementary data to this article can be found online at https://doi.org/10.1016/j.jconrel.2020.10.040.

References

[1] J. Meulemans, P. Delaere, V. Vander Poorten, Photodynamic therapy in head and neck cancer: indications, outcomes, and future prospects, Curr. Opin. Otolaryngol Head Neck Surg. 27 (2019) 136–141.
[2] P. van Driel, M.C. Boonstra, M.D. Slooter, R. Heukers, M.A. Stammes, T.J. A. Snoeks, H.S. de Bruijn, P.J. van Diest, A.L. Vahrmeijer, P.M.P. van Bergen En Henegouwen, C.J.H. van de Velde, C. Lowik, D.J. Robinson, S. Oliveira, EGFR targeted nanobody-photosensitizer conjugates for photodynamic therapy in a pre-clinical model of head and neck cancer, J. Control. Release 229 (2016) 93–105.
[3] D. van Straten, V. Mashayekhi, H.S. de Bruijn, S. Oliveira, D.J. Robinson, Oncologic photodynamic therapy: basic principles, current clinical status and future directions, Cancers. 9 (2017) 1–54.
[4] I. Yakavets, M. Millard, V. Zorin, H.P. Lassalle, L. Bezdetnaya, Current state of the nanoscale delivery systems for temoporfin-based photodynamic therapy: advanced delivery strategies, J. Control. Release 304 (2019) 268–287.
[5] R. Baskaran, J. Lee, S.G. Yang, Clinical development of photodynamic agents and therapeutic applications, Biomater. Res. 22 (2018) 1–8.
[6] M.A.M.D. Biel, Photodynamic therapy of head and neck cancer-what's old and what's new. In handbook of photodynamic therapy: updates on recent applications of porphyrin-based compounds, World Scientific (2016) 439–458.
[7] C. Hopper, Photodynamic therapy: a clinical reality in the treatment of cancer, The Lancet. Oncology. 1 (2000) 212–219.
[8] M. Chen, X. Liu, A. Fahr, Skin penetration and deposition of carboxyfluorescein and temoporfin from different lipid vesicular systems: in vitro study with finite and infinite dosage application, Int. J. Pharm. 408 (2011) 223–234.
[9] R.W. Redmond, E.J. Land, T.G. Truscott, Aggregation effects on the photophysical properties of porphyrins in relation to mechanisms involved in photodynamic therapy, Adv. Exp. Med. Biol. 193 (1985) 293–302.
[10] M. Triesscheijn, M. Ruevekamp, R. Out, T.J. Van Berkel, J. Schellens, P. Baas, F. A. Stewart, The pharmacokinetic behavior of the photosensitizer meso-tetra-hydroxyphenyl-chlorin in mice and men, Cancer Chemother. Pharmacol. 60 (2007) 113–122.
[11] T. Lammers, F. Kiessling, W.E. Hennink, G. Storm, Drug targeting to tumors: principles, pitfalls and (pre-) clinical progress, J. Control. Release 161 (2012) 175–187.
[12] A.Z. Wang, R. Langer, O.C. Farokhzad, Nanoparticle delivery of cancer drugs, Annu. Rev. Med. 63 (2012) 185–198.
[13] H. Maeda, J. Wu, T. Sawa, Y. Matsumura, K. Hori, Tumor vascular permeability and the EPR effect in macromolecular therapeutics: a review, J. Control. Release 65 (2000) 271–284.
[14] A. Varela-Moreira, Y. Shi, M.H.A.M. Fens, T. Lammers, W.E. Hennink, R. M. Schiffelers, Clinical application of polymeric micelles for the treatment of cancer, Materials Chemistry Frontiers. 1 (2017) 1485–1501.
[15] H. Cabral, K. Miyata, K. Osada, K. Kataoka, Block copolymer micelles in nanomedicine applications, Chem. Rev. 118 (2018) 6844–6892.
[16] J.W.H. Wennink, Y. Liu, P.I. Makinen, F. Setaro, A. de la Escosura, M. Bourajjaj, J. P. Lappalainen, L.P. Holappa, J.B. van den Dikkenberg, M. Al Fartousi, P. N. Trohopoulos, S. Yla-Herttuala, T. Torres, W.E. Hennink, C.F. van Nostrum, Macrophage selective photodynamic therapy by meta-tetra(hydroxyphenyl)chlorin loaded polymeric micelles: a possible treatment for cardiovascular diseases, Eur. J. Pharm. Sci. 107 (2017) 112–125.
[17] Y. Liu, L. Scrivano, J.D. Peterson, M.H.A.M. Fens, I. Beltrán Hernández, B. Mesquita, J. Sastre Torano, W.E. Hennink, C.F. van Nostrum, S. Oliveira, EGFR targeted nanobody functionalized polymeric micelles loaded with mTHPC for selective photodynamic therapy, Mol. Pharm. 17 (2020) 1276–1292.
[18] I.K. Kwon, S.C. Lee, B. Han, K. Park, Analysis on the current status of targeted drug delivery to tumors, J. Control. Release 164 (2012) 108–114.
[19] Y. Shi, R. van der Meel, B. Theek, E. Oude Blenke, E.H. Pieters, M.H. Fens, J. Ehling, R.M. Schiffelers, G. Storm, C.F. van Nostrum, T. Lammers, W.E. Hennink, Complete regression of xenograft tumors upon targeted delivery of paclitaxel via π-π stacking stabilized polymeric micelles, ACS Nano 9 (2015) 3740–3752.
[20] N. Bertrand, J.-C. Leroux, The journey of a drug-carrier in the body: an anatomo-physiological perspective, J. Control. Release 161 (2012) 152–163.
[21] C. Deng, Y. Jiang, R. Cheng, F. Meng, Z. Zhong, Biodegradable polymeric micelles for targeted and controlled anticancer drug delivery: promises, progress and prospects, Nano Today 7 (2012) 467–480.
[22] Y. Liu, M.H.A.M. Fens, B. Lou, N.C.H. van Kronenburg, R.F.M. Maas-Bakker, R. J. Kok, S. Oliveira, W.E. Hennink, C.F. van Nostrum, π-π-Stacked poly (ε-caprolactone)-b-poly(ethylene glycol) micelles loaded with a photosensitizer for photodynamic therapy, Pharmaceutics 12 (2020) 338.
[23] Y. Shi, T. Lammers, G. Storm, W.E. Hennink, Physico-chemical strategies to enhance stability and drug retention of polymeric micelles for tumor-targeted drug delivery, Macromol. Biosci. 17 (2017) 1–11.
[24] B. Liu, S. Thayumanavan, Importance of evaluating dynamic encapsulation stability of amphiphilic assemblies in serum, Biomacromolecules. 18 (2017) 4163–4170.
[25] M. Talelli, M. Barz, C.J.F. Rijcken, F. Kiessling, W.E. Hennink, T. Lammers, Core-crosslinked polymeric micelles: principles, preparation, biomedical applications and clinical translation, Nano Today 10 (2015) 93–117.
[26] S. Sasnouski, V. Zorin, I. Khludeyev, M.A. D'Hallewin, F. Guillemin, L. Bezdetnaya, Investigation of Foscan interactions with plasma proteins, Biochim. Biophys. Acta 1725 (2005) 394–402.
[27] L. Polo, G. Valduga, G. Jori, E. Reddi, Low-density lipoprotein receptors in the uptake of tumour photosensitizers by human and rat transformed fibroblasts, Int. J. Biochem. Cell Biol. 34 (2002) 10–23.
[28] R.K. Chowdhary, I. Sharif, N. Chansarkar, D. Dolphin, L. Ratkay, S. Delaney, H. Meadows, Correlation of photosensitizer delivery to lipoproteins and efficacy in tumor and arthritis mouse models; comparison of lipid-based and Pluronic P123 formulations, Journal of pharmacy & pharmaceutical sciences. 6 (2003) 198–204.
[29] V. Reshetov, V. Zorin, A. Siupa, M.A. D'Hallewin, F. Guillemin, L. Bezdetnaya, Interaction of liposomal formulations of meta-tetra(hydroxyphenyl)chlorin (temoporfin) with serum proteins: protein binding and liposome destruction, Photochem. Photobiol. 88 (2012) 1256–1264.

[30] H. Shi, W.N. Leonhard, N.J. Sijbrandi, M.J. van Steenbergen, M. Fens, J.B. van de Dikkenberg, J.S. Torano, D.J.M. Peters, W.E. Hennink, R.J. Kok, Folate-dactolisib conjugates for targeting tubular cells in polycystic kidneys, J. Control. Release 293 (2019) 113–125.
[31] S.A. Abouelmagd, B. Sun, A.C. Chang, Y.J. Ku, Y. Yeo, Release kinetics study of poorly water-soluble drugs from nanoparticles: are we doing it right? Mol. Pharm. 12 (2015) 997–1003.
[32] S.C. Owen, D.P.Y. Chan, M.S. Shoichet, Polymeric micelle stability, Nano Today 7 (2012) 53–65.
[33] W.J. Lin, L.W. Juang, C.C. Lin, Stability and release performance of a series of pegylated copolymeric micelles, Pharm. Res. 20 (2003) 668–673.
[34] M. Wagner, S. Holzschuh, A. Traeger, A. Fahr, U.S. Schubert, Asymmetric flow field-flow fractionation in the field of nanomedicine, Anal. Chem. 86 (2014) 5201–5210.
[35] Y. Liu, M.J. van Steenbergen, Z. Zhong, S. Oliveira, W.E. Hennink, C.F. van Nostrum, Dithiolane crosslinked poly(ε-caprolactone)-based micelles: impact of monomer sequence, nature of monomer and reducing agent on the dynamic crosslinking properties, Macromolecules. 53 (2020) 7009–7024.
[36] Y. Zhang, M. Huo, J. Zhou, S. Xie, PKSolver: an add-in program for pharmacokinetic and pharmacodynamic data analysis in Microsoft excel, Comput. Methods Prog. Biomed. 99 (2010) 306–314.
[37] M.G. Carstens, J.J.L. Bevernage, C.F. van Nostrum, M.J. van Steenbergen, F. M. Flesch, R. Verrijk, L.G.J. de Leede, D.J.A. Crommelin, W.E. Hennink, Small oligomeric micelles based on end group modified mPEG−oligocaprolactone with monodisperse hydrophobic blocks, Macromolecules. 40 (2007) 116–122.
[38] R.K. O'Reilly, C.J. Hawker, K.L. Wooley, Cross-linked block copolymer micelles: functional nanostructures of great potential and versatility, Chem. Soc. Rev. 35 (2006) 1068–1083.
[39] G. Gaucher, M.H. Dufresne, V.P. Sant, N. Kang, D. Maysinger, J.C. Leroux, Block copolymer micelles: preparation, characterization and application in drug delivery, J. Control. Release 109 (2005) 169–188.
[40] L. Glavas, P. Olsen, K. Odelius, A.C. Albertsson, Achieving micelle control through core crystallinity, Biomacromolecules. 14 (2013) 4150–4156.
[41] J. Zhang, L.-Q. Wang, H. Wang, K. Tu, Micellization phenomena of amphiphilic block copolymers based on methoxy poly(ethylene glycol) and either crystalline or amorphous poly(caprolactone-b-lactide), Biomacromolecules. 7 (2006) 2492–2500.
[42] G. Bastiat, C.O. Pritz, C. Roider, F. Fouchet, E. Lignieres, A. Jesacher, R. Glueckert, M. Ritsch-Marte, A. Schrott-Fischer, P. Saulnier, J.P. Benoit, A new tool to ensure the fluorescent dye labeling stability of nanocarriers: a real challenge for fluorescence imaging, J. Control. Release 170 (2013) 334–342.
[43] C. Rijcken, Tuneable & Degradable Polymeric Micelles for Drug Delivery: From Synthesis to Feasibility In Vivo, Utrecht University, Utrecht, Doctoral dissertation, 2007, pp. 239–260.
[44] O. Soga, Biodegradable Thermosensitive Polymers: Synthesis, Characterization and Drug Delivery Applications,, Utrecht University, Utrecht, Doctoral dissertation, 2006, pp. 87–102.
[45] A.T. Michael-Titus, R. Whelpton, Z. Yaqub, Binding of temoporfin to the lipoprotein fractions of human serum, Br. J. Clin. Pharm. 40 (1995) 594–597.
[46] C. Decker, H. Schubert, S. May, A. Fahr, Pharmacokinetics of temoporfin-loaded liposome formulations: correlation of liposome and temoporfin blood concentration, J. Control. Release 166 (2013) 277–285.
[47] N. Kamaly, Z. Xiao, P.M. Valencia, A.F. Radovic-Moreno, O.C. Farokhzad, Targeted polymeric therapeutic nanoparticles: design, development and clinical translation, Chem. Soc. Rev. 41 (2012) 2971–3010.